### *4.5.4 Stabilization of Microtubules*

In tauopathy model(s), misfolded mutant tau protein causes axonal dysfunction/degeneration [39]. Microtubule-binding drugs can be therapeutically beneficial in tauopathy models by functionally substituting for the microtubule-binding protein tau, which is sequestered into inclusions of human tauopathies and transgenic mouse models [39]. Mutant tau transgenic mice treated with paclitaxel (Paxceed) showed that fast axonal transport in spinal axons is restored, and that microtubule numbers and stable tubulins are increased compared with sham treatment [39]. Moreover, Paxceed ameliorated motor impairments in tau transgenic mice [39]. Thus, microtubule-stabilizing drugs have therapeutic potential for axonal dysfunction/degeneration, in tauopathies by offsetting losses of tau function that result from the sequestration of this microtubule-stabilizing protein into filamentous misfolded inclusions [39].

## 4.6 Concluding Remarks

Accumulating experimental evidence suggests that protection/functional repair of axons (Fig. 4.5) can be a general therapeutic strategy for neuronal dysfunction caused by misfolded protein(s) deposition in neurodegenerative disease(s). The translation of these results into human disease therapies should be done in the near future.

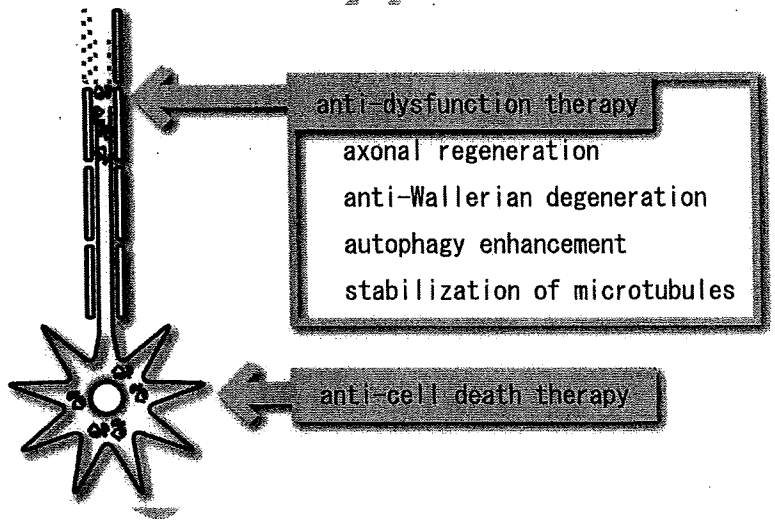


**Fig. 4.5** Anti-dysfunction therapy for axonal protection and anti-cell death therapy for inhibiting neuronal loss. Neuronal dysfunction in neurodegeneration is reversible. Axonal regeneration, anti-Wallerian degeneration, autophagy enhancement, and/or stabilization of microtubules may be effective as anti-dysfunction therapies by protecting axon from neurodegenerative diseases, although anti-cell death therapies may inhibit only neuronal cell body loss

## Abbreviations

amyotrophic lateral sclerosis (ALS)
alpha-amino-3-hydroxy-5-methyl-4-isoxazolepropionic acid (AMPA)
adaptor protein-4 (AP-4)
EGF receptor (EGFR)
Huntington's disease (HD)
*N*-methyl-4-phenyl-1,2,3,6-tetrahydropyridine (MPTP)
mammalian target of rapamycin (mTOR)
Parkinson's disease (PD)
progressive motor neuronopathy (*pmn*)
transmembrane AMPA receptor regulatory protein (TARP)
leucine-rich repeat Ig-containing protein (LINGO-1)
Wallerian degeneration slow (*Wlds*)

## References

1. Palop JJ, Chin J, Mucke L (2006) A network dysfunction perspective on neurodegenerative diseases. Nature 443:768–773
2. Yamamoto A, Lucas JJ, Hen R (2000) Reversal of neuropathology and motor dysfunction in a conditional model of Huntington's disease. Cell 101:57–66
3. Orr HT, Zoghbi HY. (2000) Reversing neurodegeneration: a promise unfolds. Cell 101:1–4
4. Wang J, Wang C-E, Orr A, Tydlacka S, Li S-H, Li X-J (2008) Impaired ubiquitin – proteasome system activity in the synapses of Huntington's disease mice. J Cell Biol 180:1177–1189
5. Eberhardt O,Coelln RV, Kugler S, Lindenau J, Rathke-Hartlieb S, Gerhardt E, Haid S, Isenmann S, Gravel C, Srinivasan A et al. (2000) Protection by synergistic effects of adenovirus-mediated X chromosome-linked inhibitor of apoptosis and glial cell line-derived neurotrophic factor gene transfer in the 1-methyl-4-phenyl-1,2,3,6-tetrahydropyridine model of Parkinson's disease. J Neurosci 20:9126–9134
6. Vila M, Jackson-Lewis V, Vukosavic S, Djaldetti R, Liberatore G, Offen D, Korsmeyer SJ, Przedborski S (2001) Bax ablation prevents dopaminergic neurodegeneration in the 1-methyl-4-phenyl-1,2,3,6-tetrahydropyridine mouse model of Parkinson's disease. Proc Natl Acad Sci USA 98:2837–2842
7. Inoue H, Tsukita K, Iwasato T, Suzuki Y, Tomioka M, Tateno M, Nagao M, Kawata A, Saido TC, Miura M et al. (2003) The crucial role of caspase-9 in the disease progression of a transgenic ALS mouse model. EMBO J 22:6665–6674
8. Gould TW, Buss RR, Vinsant S, Prevette D, Sun W, Knudson CM, Milligan CE, Oppenheim (2006) Complete dissociation of motor neuron death from motor dysfunction by Bax deletion in a mouse model of ALS. J Neurosci 26:8774–8786
9. Fischer LR, Glass JD (2007) Axonal degeneration in motor neuron disease. Neurodegener Dis 4:431–442
10. Sagot Y, Vejsada R, Kato A (1997) Clinical and molecular aspects of motoneurone diseases: animal models, neurotrophic factors and Bcl-2 oncoprotein. Trends Pharmacol Sci 18:330–337
11. Finn JT, Weil M, Archer F, Siman R, Srinivasan A, Raff MC (2000) Evidence that Wallerian degeneration and localized axon degeneration induced by local neurotrophin deprivation do not involve caspases. J Neurosci 20:1333–1341
12. Orimo S, Uchihara T, Nakamura A, Mori F, Kakita A, Wakabayashi K, Takahashi H (2008) Axonal α-synuclein aggregates herald centripetal degeneration of cardiac sympathetic nerve in Parkinson's disease. Brain 131:642–650

13. Bradley WG, Good P, Rasool CG, Adelman LS (1983) Morphometric and biochemical studies of peripheral nerves in amyotrophic lateral sclerosis. Ann Neurol 14:267–277
14. Fischer LR, Culver DG, Tennant P, Davis AA, Wang M, Castellano-Sanchez A, Khan J, Polak MA, Glass JD (2004) Amyotrophic lateral sclerosis is a distal axonopathy: evidence in mice and man. Exp Neurol 185:232–240
15. Kanai K, Kuwabara S, Misawa S, Tamura N, Ogawara K, Nakata M, Sawai S, Hattori T, Bostock H (2006) Altered axonal excitability properties in amyotrophic lateral sclerosis: impaired potassium channel function related to disease stage. Brain 129:953–962
16. Vucic S, Kiernan MC (2006) Axonal excitability properties in amyotrophic lateral sclerosis. Clin Neurophysiol 117:1458–1466
17. Nakata M, Kuwabara S, Kanai K, Misawa S, Tamura N, Sawai S, Hattori T, Bostock H (2006) Distal excitability changes in motor axons in amyotrophic lateral sclerosis. Clin Neurophysiol 117:1444–1448
18. Pasinelli P, Brown RH (2006) Molecular biology of amyotrophic lateral sclerosis: insights from genetics. Nat Rev Neurosci 7:710–723
19. Coleman M (2005) Axon degeneration mechanisms: commonality amid diversity. Nat Rev Neurosci 6:889–898
20. Hara T, Nakamura K, Matsui M, Yamamoto A, Nakahara Y, Suzuki-Migishima R, Yokoyama M, Mishima K, Saito I, Okano H et al. (2006) Suppression of basal autophagy in neural cells causes neurodegenerative disease in mice. Nature 441:885–889
21. Komatsu M, Waguri S, Chiba T, Murata S, Iwata J, Tanida I, Ueno T, Koike M, Uchiyama Y, Kominami E et al. (2006) Loss of autophagy in the central nervous system causes neurodegeneration in mice. Nature 441:880–884
22. Komatsu M, Wang QJ, Holstein GR, Friedrich VL Jr, Iwata J, Kominami E, Chait BT, Tanaka K, Yue Z. (2007) Essential role for autophagy protein Atg7 in the maintenance of axonal homeostasis and the prevention of axonal degeneration. Proc Natl Acad Sci USA 104: 14489–14494
23. Mizushima N, Levine B, Cuervo AM, Klionsky DJ (2008) Autophagy fights disease through cellular self-digestion. Nature 451:1069–1075
24. Komatsu M, Waguri S, Koike M, Sou Y, Ueno T, Hara T, Mizushima N, Iwata J, Ezaki J, Murata S et al. (2007) Homeostatic levels of p62 control cytoplasmic inclusion body formation in autophagy-deficient mice. Cell 131:1149–1163
25. Matsuda S, Miura E, Matsuda K, Kakegawa W, Kohda K, Watanabe M, Yuzaki M (2008) Accumulation of AMPA receptors in autophagosomes in neuronal axons lacking adaptor protein AP-4. Neuron 57:730–745
26. Inoue H, Lin L, Lee X, Shao Z, Mendes S, Snodgrass-Belt P, Sweigard H, Engber T, Pepinsky B, Yang L et al. (2007) Inhibition of the leucine-rich repeat protein LINGO-1 enhances survival, structure, and function of dopaminergic neurons in Parkinson's disease models. Proc Natl Acad Sci USA 104:14430–14435
27. Bandtlow C, Dechant G (2004) From cell death to neuronal regeneration, effects of the p75 neurotrophin receptor depend on interactions with partner subunits. Sci STKE 235:pe24
28. Mi S, Sandrock A, Miller RH (2008) LINGO-1 and its role in CNS repair. Int J Biochem Cell Biol. doi:10.1016/j.biocel.2008.03.018
29. Wang J, So K-F, McCoy JM, Pepinsky RB, Mi S, Relton JK (2006) LINGO-1 antagonist promotes functional recovery and axonal sprouting after spinal cord injury. Mol Cell Neurosci 33:311–320
30. Trifunovski A, Josephson A, Ringman A, Brene S, Spenger C, Olson L (2004) Neuronal activity-induced regulation of Lingo-1. Neuroreport 15:2397–2400
31. Araki T, Sasaki Y, Milbrandt J (2004) Increased nuclear NAD biosynthesis and SIRT1 activation prevent axonal degeneration. Science 305:1010–1013
32. Sajadi A, Schneider BL, Aebischer P (2004) WldS-mediated protection of dopaminergic fibers in an animal model of Parkinson disease. Curr Biol 14:326–330
33. Mi W, Beirowski B, Gillingwater TH, Adalbert R, Wagner D, Grumme D, Osaka H, Conforti L, Arnhold S, Addicks K et al. (2005) The slow Wallerian degeneration gene, *WldS*, inhibits axonal spheroid pathology in gracile axonal dystrophy mice. Brain 128:405–416

AQ1

34. Fischer LR, Culver DG, Davis AA, Tennant P, Wang M, Coleman M, Asress S, Adalbert R, Alexander GM, Glass JD (2005) The *WldS* gene modestly prolongs survival in the SOD1G93A fALS mouse. Neurobiol Dis 19:293–300
35. Vande Velde C, Garcia ML, Yin X, Trapp BD, Cleveland DW (2004) The neuroprotective factor WldS does not attenuate mutant SOD1-mediated motor neuron disease. Neuromolecular Med 5:193–204
36. Ravikumar B, Vacher C, Berger Z, Davies JE, Luo S, Oroz LG, Scaravilli F, Easton DF, Duden R, O'Kane CJ et al. (2004) Inhibition of mTOR induces autophagy and reduces toxicity of polyglutamine expansions in fly and mouse models of Huntington disease. Nat Genet 36: 585–595
37. Sarkar S, Perlstein EO, Imarisio S, Pineau S, Cordenier A, Maglathlin RL, Webster JA, Lewis TA, O'Kane CJ, Schreiber SL et al. (2007) Small molecules enhance autophagy and reduce toxicity in Huntington's disease models. Nat Chem Biol 3:331–338
38. Ehninger D, Han S, Shilyansky C, Zhou Y, Li W, Kwiatkowski DJ, Ramesh V, Silva AJ (2008) Reversal of learning deficits in a Tsc2 + /− mouse model of tuberous sclerosis. Nat Med. doi:10.1038/nm1788
39. Zhang B, Maiti A, Shively S, Lakhani F, McDonald-Jones G, Bruce J, Lee E B, Xie S X, Joyce S, Li C et al. (2005) Microtubule-binding drugs offset tau sequestration by stabilizing microtubules and reversing fast axonal transport deficits in a tauopathy model. Proc Natl Acad Sci USA 102:227–231

AQ2

# Chapter-4

| Query No. | Page No. | Line No. | Query |
|---|---|---|---|
| AQ1 | 108 | 18 | Please provide volume and page range details for the reference (28). |
| AQ2 | 108 | 41 | Please provide volume and page range details for the reference (38). |

*Journal of Neurochemistry*, 2007, **102**, 1497–1505 doi:10.1111/j.1471-4159.2007.04534.x

# Heat-shock protein 105 interacts with and suppresses aggregation of mutant Cu/Zn superoxide dismutase: clues to a possible strategy for treating ALS

Hirofumi Yamashita,*,† Jun Kawamata,* Katsuya Okawa,‡ Rie Kanki,* Tomoki Nakamizo,* Takumi Hatayama,§ Koji Yamanaka,† Ryosuke Takahashi* and Shun Shimohama*,¶

**Department of Neurology, Kyoto University Graduate School of Medicine, Kyoto, Japan*

*†Yamanaka Research Unit, RIKEN Brain Science Institute, Wako, Japan*

*‡Horizontal Medical Research Organization, Kyoto University Graduate School of Medicine, Kyoto, Japan*

*§Department of Biochemistry, Kyoto Pharmaceutical University, Kyoto, Japan*

*¶Department of Neurology, Sapporo Medical University School of Medicine, Sapporo, Japan*

**Abstract**

A dominant mutation in the gene for copper-zinc superoxide dismutase (SOD1) is the most frequent cause of the inherited form of amyotrophic lateral sclerosis. Mutant SOD1 provokes progressive degeneration of motor neurons by an unidentified acquired toxicity. Exploiting both affinity purification and mass spectrometry, we identified a novel interaction between heat-shock protein 105 (Hsp105) and mutant SOD1. We detected this interaction both in spinal cord extracts of mutant $SOD1^{G93A}$ transgenic mice and in cultured neuroblastoma cells. Expression of Hsp105, which is found in mouse motor neurons, was depressed in the spinal cords of $SOD1^{G93A}$ mice as disease progressed, while levels of expression of two other heat-shock proteins, Hsp70 and Hsp27, were elevated. Moreover, Hsp105 suppressed the formation of mutant SOD1-containing aggregates in cultured cells. These results suggest that techniques that raise levels of Hsp105 might be promising tools for alleviation of the mutant SOD1 toxicity.

**Keywords:** amyotrophic lateral sclerosis, Cu/Zn superoxide dismutase (or superoxide dismutase 1), heat-shock protein 105.

*J. Neurochem.* (2007) **102**, 1497–1505.

Amyotrophic lateral sclerosis (ALS) is an adult-onset neurodegenerative disease causing the selective loss of motor neurons, which results in progressive and ultimately fatal paralysis of skeletal muscles. Death usually occurs within 2–5 years after onset of the disease and is related to respiratory-muscle weakness. Ten percent of cases of ALS are inherited, and the most frequent cause of inherited ALS is dominant mutations in the gene for Cu/Zn superoxide dismutase (SOD1). More than 100 different mutations in SOD1 have been identified, all of which provoke uniform disease phenotype that is similar to the phenotype of the sporadic disease. Transgenic mice and rats expressing a mutant human gene for SOD1 develop an ALS phenotype, although deletion of SOD1 from mice does not cause motor neuron disease, providing evidence for acquired toxicity due to mutant SOD1 (Bendotti and Carri 2004; Bruijn *et al.* 2004).

Several hypotheses have been proposed to explain the mechanism of mutant SOD1-mediated toxicity, including formation of protein aggregates due to reduced conformational stability, mitochondrial dysfunction, excitotoxicity, abnormal axonal transport, mutant-derived oxidative damage, lack of growth factors, and inflammation. However, the exact mechanism responsible for motor neuron degeneration remains unknown. One plausible hypothesis is linked to the

Received November 30, 2006; revised manuscript received February 08, 2007; accepted February 14, 2007.

Address correspondence and reprint requests to Dr Shun Shimohama, Department of Neurology, Sapporo Medical University School of Medicine, S1 W16, Chuo-ku, Sapporo 060-8543, Japan.
E-mail: shimoha@sapmed.ac.jp

*Abbreviations used:* ALS, amyotrophic lateral sclerosis; HRP, horseradish peroxidase; HEK, human embryonic kidney; HSF, heat shock factor; IP, immunoprecipitation; MALDI-TOF, matrix-assisted laser desorption/ionization time-of-flight; MS, mass spectrometry; PBS, phosphate-buffered saline; SDS–PAGE, sodium dodecyl sulfate–polyacrylamide gel electrophoresis; SOD, superoxide dismutase; WT, wild-type.

 

impairment of protein-quality control. Accumulation of mutant SOD1 might result in (i) saturation of the protein-folding and protein-degradation machinery that handles mutant proteins and/or (ii) disruption of vital intracellular processes by misfolded, oligomeric species of SOD1. In such cases, it is likely that mutant SOD1 might provoke toxicity through abnormal interactions between mutant SOD1 and other proteins. In this context, identification of proteins that interact with mutant SOD1 might provide clues to the toxic effects of the mutant protein. Mutant but not wild-type (WT) SOD1 has been found to interact with proteins that are involved in protein-quality control, for example, several heat-shock proteins such as Hsp70 (Shinder *et al.* 2001; Okado-Matsumoto and Fridovich 2002), Hsp40, αB-crystallin (Shinder *et al.* 2001), and Hsp27 (Okado-Matsumoto and Fridovich 2002) and E3 ligases such as dorfin (Niwa *et al.* 2002), NEDL1 (Miyazaki *et al.* 2004), and carboxy terminus of the Hsc70-interacting protein (Choi *et al.* 2004; Urushitani *et al.* 2004).

Abnormal expression of heat-shock proteins has been detected in mutant SOD1 mouse models. Increased expression of Hsp70 in mutant SOD1-expressing fibroblasts (Bruening *et al.* 1999) and of Hsp27 (also referred to as Hsp25) in spinal cord lysates of symptomatic $SOD1^{G93A}$ mice (Vleminckx *et al.* 2002) has been reported, but decreased expression of Hsp27 has also been found in motor neurons from symptomatic $SOD1^{G93A}$ mice (Maatkamp *et al.* 2004). Hsp70/Hsc70 were found in aggregates of mutant SOD1 in the motor neurons of symptomatic mutant SOD1 mice (Watanabe *et al.* 2001; Liu *et al.* 2005). These findings support the hypothesis that depletion of chaperone proteins might be responsible for the toxicity of mutant SOD1. Over-expression of Hsp70 in mutant SOD1 mice did not reverse the disease process (Liu *et al.* 2005), whereas activation of heat shock factor (HSF)-1, a transcription factor for heat-shock proteins, by administration of arimoclomol extended the life span of mutant SOD1 mice (Kieran *et al.* 2004). Such observations suggest that modulation of heat-shock responses might be an attractive strategy for treatment of motor neuron disease. Thus, it seems appropriate to elucidate the mechanism(s) of misregulation of heat-shock proteins that is linked to mutant SOD1-mediated toxicity, which remains poorly understood.

To uncover the properties of mutant SOD1 as they relate to protein-quality control, we investigated the proteins that interact with mutant SOD1 by immunoprecipitation (IP) and subsequent mass spectrometric (MS) analysis. We identified heat-shock protein 105 (Hsp105) as a novel mutant SOD1-interacting protein, and we detected this interaction in spinal cord extracts of mutant $SOD1^{G93A}$ transgenic mice. Levels of expression of Hsp105, which is detected in mouse motor neurons, were depressed in the spinal cords of $SOD1^{G93A}$ mice during disease progression, although levels of expression of other heat-shock protein rose. In addition, Hsp105 suppressed the aggregation of mutant SOD1 in cultured cells. Together, our findings indicate that raising levels of Hsp105 may alleviate the mutant SOD1-mediated toxicity.

## Materials and methods

### Plasmids

The coding region of human WT SOD1 cDNA was cloned into the expression vector pcDNA3.1(+) (Invitrogen, Carlsbad, CA, USA) and various mutations in SOD1 were generated (Oeda *et al.* 2001) by site-directed mutagenesis using a Mutan™-Super Express Km kit (Takara, Otsu, Japan), in accordance with the manufacturer's instruction. Then a FLAG tag was introduced at the carboxyl terminus of SOD1 and its mutant derivatives by PCR. A fragment of cDNA encoding mouse Hsp105 (Yasuda *et al.* 1995) was cloned into the pcDNA4/TO vector (Invitrogen).

### Antibodies

The primary antibodies used for immunoblots or IP included anti-SOD1 antibody (Stressgen Biotechnologies, Victoria, BC, Canada), anti-FLAG antibody (M2; Sigma, St Louis, MO, USA), anti-β-actin antibody (Sigma), mouse anti-Hsp105 antibody (BD Biosciences, San Jose, CA, USA), anti-Hsp70 antibody (Santa Cruz Biotechnology, Santa Cruz, CA, USA), anti-Hsp27 antibody (Santa Cruz Biotechnology), and anti-β-galactosidase antibody (Chemicon, Temecula, CA, USA). For immunofluorescence staining, we used rabbit anti-Hsp105 antibody (Stressgen Biotechnologies) and SMI32 antibody (Sternberger Monoclonals, Baltimore, MA, USA). Secondary antibodies for immunoblots were anti-rabbit IgG conjugated with horseradish peroxidase (HRP; GE Healthcare, Piscataway, NJ, USA), anti-mouse IgG conjugated with HRP (GE Healthcare), and anti-goat IgG conjugated with HRP (Santa Cruz Biotechnology).

### Culture and transfection of cells

Neuro2A and human embryonic kidney (HEK)293T cells were maintained in Dulbecco's modified Eagle's medium, supplemented with 10% fetal bovine serum, 100 IU/mL penicillin, 100 μg/mL streptomycin, and 2 mmol/L glutamine. Cells were transiently transfected with Lipofectamine™ 2000 (Invitrogen) according to the manufacturer's instruction. After 24 h, cells were harvested and cellular proteins were subjected to IP or immunoblotting.

### Transgenic mice

Mutant (B6SJL-TgN [SOD1-G93A] 1Gur) and WT (B6SJL-Tg [SOD1] 2Gur/J) SOD1 transgenic mice were obtained from the Jackson Laboratory (Bar Harbor, ME, USA). Mice were genotyped by PCR with the following sense and antisense primers: 5′-CATCAGCCCTAATCCATCTGA-3′ and 5′-CGCGACTAACAAT-CAAAGTGA-3′, respectively. Mice were housed and treated in compliance with the 'Guidelines for Animal Experiments' of Kyoto University, Japan.

### Preparation of lysates and IP of proteins

Lysates were prepared, on ice, from cells or tissue in lysis buffer (10 mmol/L Tris–HCl, pH 7.8, 1% Nonidet P-40, 0.15 mol/L NaCl, 1 mmol/L EDTA, and 10 μg/mL aprotinin). After centrifugation (21 600 *g*, 30 min, 4°C), the clarified supernatants were used for

 

subsequent analysis unless specified. Protein concentrations were determined by Bradford's assay (Bio-Rad, Hercules, CA, USA). For IP, aliquots of 600 μg of protein in 1000 μL of lysis buffer were incubated for 12 h at 4°C with protein G-Sepharose (GE Healthcare). Then they were incubated with rabbit anti-SOD1 (3 μg) or mouse anti-FLAG antibodies (8.8 μg) or normal IgG for 1 h. The antibody–antigen complexes were then incubated with 10 μL of protein G-Sepharose for another hour. After immunoprecipitates had been washed five times with 1000 μL of lysis buffer, protein complexes were eluted with 15 μL of sample buffer for sodium dodecyl sulfate–polyacrylamide gel electrophoresis (SDS–PAGE) (0.125 mol/L Tris–HCl, pH 6.8, 4% SDS, 20% glycerol, 20 mmol/L dithiothreitol, and 0.002% bromo phenol blue) and immediately boiled for 5 min. Supernatants, after clarification by centrifugation, were loaded on a 2–15% polyacrylamide gradient gel (PAGmini; Daiichi Pure Chemicals, Tokyo, Japan) for SDS–PAGE.

### Immunoblotting

Lysates prepared in lysis buffer or the whole tissue homogenates, which were prepared by homogenization of spinal cord with the equal volume of SDS sample buffer, were fractionated with SDS–PAGE, then transferred to a polyvinylidene difluoride membrane (Millipore Corporation, Bedford, MA, USA). Membranes were incubated with primary antibodies and appropriate HRP-conjugated secondary antibodies. Immunoreactive proteins on membranes were visualized with the enhanced chemiluminescence western blotting detection reagents (GE Healthcare).

### MS

Proteins were identified by MS as described previously (Jensen *et al.* 1996). In brief, after SDS–PAGE, proteins were visualized by silver staining (PlusOne; GE Healthcare) and bands of proteins were excised from gels. After overnight in-gel digestions at 37°C of proteins with trypsin in a buffer that contained 50 mmol/L ammonium bicarbonate (pH 8.0) and 2% acetonitrile, molecular-mass analysis of tryptic peptides was performed by matrix-assisted laser desorption/ionization time-of-flight MS (MALDI-TOF/MS) with an Ultraflex MALDI-TOF/TOF system (Bruker Daltonics, Billerica, MA, USA). The acquired mass spectral data were queried against the National Center for Biotechnology Information non-redundant database using the Mascot (Matrix Science, London, UK) search engine with a peptide mass tolerance of 0.15 Da and allowance for up to two trypsin miscleavages.

### Filter trap assay

Filtration of lysates through a cellulose acetate membrane (0.2-μm pores; Advantec, Dublin, CA, USA) was performed with a 96-well dot-blot apparatus (Bio-Rad) as described previously (Wang *et al.* 2002a) with minor modifications. In brief, HEK293T cells were cultured on 35-mm dishes to 70–80% confluence. Cells were co-transfected with 0.6 μg of empty vector or of plasmids encoding LacZ or Hsp105, together with 1 μg of plasmid encoding $SOD1^{G93A}$-FLAG. After incubation for 48 h, cells were harvested with phosphate-buffered saline (PBS) and briefly sonicated. Lysates were centrifuged at 800 *g* for 10 min at 4°C and the concentrations of proteins in the supernatants were determined. Aliquots of 200 μg of protein in 400 μL of lysis buffer (PBS, 1% SDS) were gently vacuum-filtered through a membrane. Membranes were washed twice with tris-buffered saline-0.05% Tween20 and analyzed by immunoblotting.

### Immunofluorescence staining

For immunofluorescence staining, mice were deeply anesthetized with pentobarbital and perfused transcardially with 4% *p*-formaldehyde in PBS. The lumbar spinal cord was dissected out, fixed overnight in 4% *p*-formaldehyde in PBS, and cryoprotected with 30% sucrose in PBS before freezing. Ten-micron cryosections were mounted on slides. After blocking with blocking buffer (5% normal goat serum and 0.3% Triton X-100 in PBS) for half an hour at 25°C, the sections were incubated overnight at 4°C with a mixture of mouse SMI32 antibody (1 : 4000) and rabbit anti-Hsp105 antibody (1 : 100). Bound antibodies were detected with Alexa Fluor 488-conjugated anti-rabbit IgG and Alexa Fluor 594-conjugated anti-mouse IgG antibodies (1 : 1000; Molecular Probes, Eugene, OR, USA). Double-immunostained fluorescent images were recorded with a Leica DMRXA2 confocal microscope (Leica, Wetzlar, Germany).

### Statistical analysis

Signals on films were quantified with NIH image software (National Institutes of Health, Bethesda, MD, USA). Statistical significance was assessed by one-way ANOVA followed by Scheffe's *post hoc* test using the KaleidaGraph program (Synergy Software, Reading, PA, USA). Statistical significance was set at a probability value of less than 0.05.

## Results

### Identification of proteins that interact with mutant SOD1 in Neuro2A cells by MALDI-TOF/MS

We attempted to identify proteins that interact specifically with ALS-associated mutant SOD1 proteins by IP and subsequent MS analysis, as illustrated in Fig. 1a. We transfected Neuro2A cells transiently with plasmids that encoded $SOD1^{WT}$-FLAG, $SOD1^{G85R}$-FLAG, or $SOD1^{G93A}$-FLAG. After 24 h, proteins in lysates from transfected Neuro2A cells were immunoprecipitated with anti-FLAG antibody or control mouse IgG. The immunoprecipitates were fractionated by SDS–PAGE, which was followed by silver staining (Figs 1b and c). We considered all bands in lanes 1, 5, and 6 to represent non-specifically interacting proteins, as they were generated in the absence of mutant SOD1 (lane 1), in the presence of control IgG (lane 5), or in the absence of antibody for IP (lane 6). We detected bands of a protein of ~19 kDa in lanes 2 and 4 and of a protein of ~18 kDa in lane 3, each of which was confirmed to be exogenous SOD1-FLAG by immunoblotting (data not shown). We identified two specific bands of proteins of approximately 70 kDa (p70) and 105 kDa (p105), respectively, that were visualized exclusively in both lanes 3 and 4 (Figs 1b and c). These two bands were excised and subjected to MALDI-TOF/MS analysis. A search for a protein similar to p70 gave 28 matches (*m/z*; 1081.53, 1197.57, 1199.59,

 

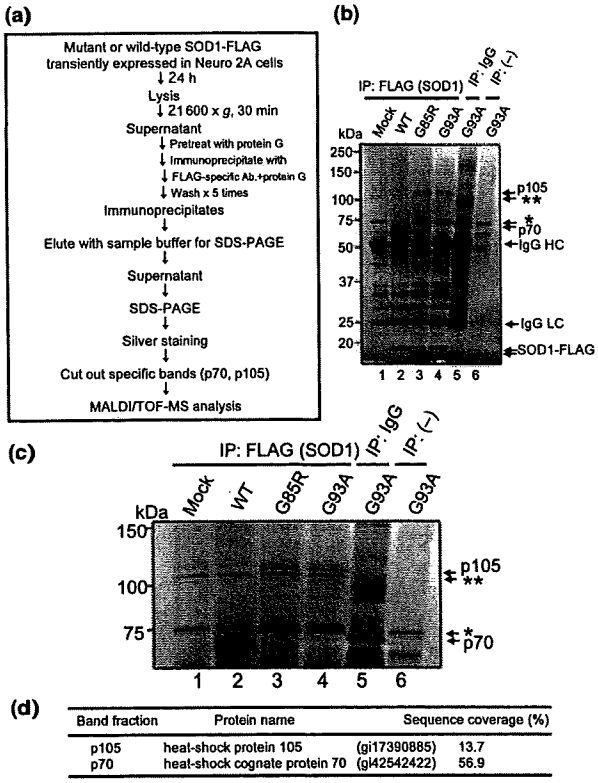


(d)

| Band fraction | Protein name | | Sequence coverage (%) |
|---|---|---|---|
| p105 | heat-shock protein 105 | (gi17390885) | 13.7 |
| p70 | heat-shock cognate protein 70 | (gi42542422) | 56.9 |

**Fig. 1** Identification of amyotrophic lateral sclerosis-associated mutant superoxide dismutase 1 (SOD1) -interacting proteins by sodium dodecyl sulfate–polyacrylamide gel electrophoresis (SDS–PAGE) and matrix-assisted laser desorption/ionization time-of-flight mass spectrometry (MALDI-TOF/MS) analysis. (a) Scheme for the experiments designed to identify proteins that interact with mutant SOD1. (b and c) Mutant SOD1-interacting proteins, as visualized by silver staining. Arrows indicate interacting proteins (p70 and p105 in lanes 3 and 4), IgG heavy chain (HC), IgG light chain (LC), and FLAG-tagged human SOD1 (lanes 2–4). The G85R mutant form of SOD1 migrates faster than the wild type (lane 3). Asterisks (* and **) denote nonspecific bands. Figure 1c shows an enlarged view of the region of the photograph that includes proteins of 50–150 kDa proteins in Fig. 1b. Two proteins that interacted specifically with mutant SOD1 are apparent (p70 and p105; lanes 3 and 4). The mobilities of these correspond to molecular masses of ~70 kDa (p70) and ~105 kDa (p105), respectively. These two bands were excised and were prepared for MS analysis. (d) MS analysis of the excised proteins in Fig. 1c. Percentage sequence coverage of each protein is shown.

1228.55, 1235.54, 1252.59, 1253.56, 1391.67, 1410.62, 1480.71, 1481.77, 1487.67, 1616.76, 1649.78, 1653.81, 1659.84, 1691.73, 1787.97, 1805.86, 1837.97, 1952.04, 1981.99, 2206.09, 2260.13, 2514.34, 2774.37, 2911.63, and 2997.52) with Hsc70 (heat-shock cognate protein 70) with 56.9% sequence coverage. In the analysis of p105, although the sequence coverage (13.7%) was lower than that of p70, 10 peaks of the theoretical mass fingerprint of Hsp105 (heat-shock protein 105) matched with the mass observed (*m/z*; 1133.56, 1321.62, 1388.67, 1479.70, 1481.75, 1487.75, 1562.77, 1637.78, 2035.13, and 2111.03) (Fig. 1d).

Those data highly suggested Hsc70 was interacted with mutant SOD1 proteins as previously reported (Shinder *et al.* 2001). More interestingly, the MS analysis also suggested a novel interaction between Hsp105 and mutant SOD1, which required further confirmation.

### Interaction of mutant SOD1 with Hsp105 both in cultured neuroblastoma cells and in mouse spinal cord

Having identified a possible novel interaction between Hsp105 and mutant SOD1, we decided to investigate the role of Hsp105 in the toxicity of mutant SOD1. We first confirmed the interaction between different mutant forms of SOD1 and endogenous Hsp105 in Neuro2A cells. We transiently transfected Neuro2A cells with plasmids that expressed FLAG-tagged SOD1 (WT) and its mutant derivatives (D96N, D90A, G85R, and G93A). Then we immunoprecipitated proteins in lysates with anti-FLAG antibody. Immunoprecipitated proteins were examined by immunoblotting for the presence of Hsp105 (Fig. 2a, upper panel) and SOD1-FLAG (Fig. 2a, second panel). Only G85R and G93A mutant forms of SOD1, which cause motor neuron disease as a dominant trait, interacted with Hsp105; WT SOD1, D96N, and D90A mutant forms of SOD1 did not. The lack of interaction of $SOD1^{D90A}$ and $SOD1^{D96N}$ with Hsp105 suggested the lower toxicity of those mutants. This observation reflects the facts that $SOD1^{D90A}$ causes motor neuron disease as a mainly recessive trait (Andersen *et al.* 1996) and that the D96N mutation has been reported as a non-disease-associated mutation, though controversial (Hand *et al.* 2001; Parton *et al.* 2001).

Next, we used mouse tissue to examine whether the interaction between mutant SOD1 and Hsp105 might occur *in vivo*. Lysates of spinal cord and of liver cells from non-transgenic, $SOD1^{WT}$ and $SOD1^{G93A}$ mice were treated with anti-SOD1 antibody and immunoprecipitates were examined for the presence of Hsp105 (Fig. 2b, upper panel) and SOD1 (Fig. 2b, second panel). In spinal cord extracts, $SOD1^{G93A}$ co-immunoprecipitated with Hsp105 (lane 3), while $SOD1^{WT}$ interacted with Hsp105 at a lower level (lane 2). No evident interaction between SOD1 and Hsp105 was detected in liver, a tissue that is not affected in ALS.

Although it has been reported that Hsp105 is expressed in brain at higher levels (Lee-Yoon *et al.* 1995; Yasuda *et al.* 1995), the cell type(s) that expresses Hsp105 in the spinal cord is unknown. We examined whether Hsp105 is expressed in motor neurons by immunofluorescence staining of spinal cord from non-transgenic mice. Motor neurons that were immunostained with the SMI32 antibody were immunopositive for Hsp105 (Fig. 2c, arrowheads), whereas non-motor neurons were also stained with anti-Hsp105 antibody (Fig. 2c, arrows). Within the motor neurons, Hsp105 was mainly localized in the cytoplasm, as is SOD1.

 

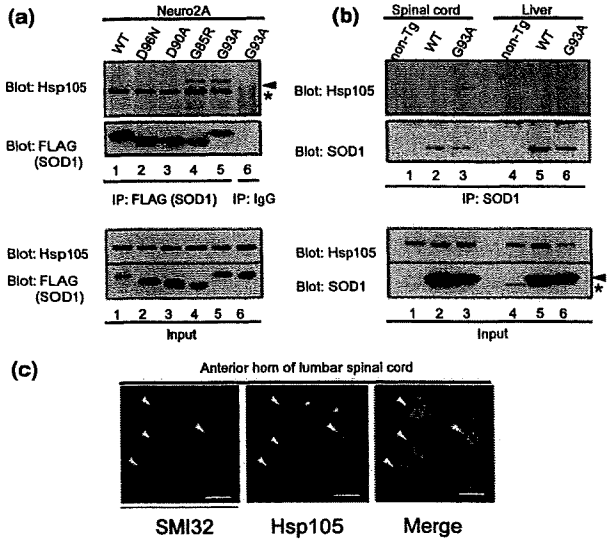


**Fig. 2** Hsp105 interacts with mutant superoxide dismutase 1 (SOD1) both in neuroblastoma cells in culture and in mouse spinal cord. (a) Lysates of Neuro2A cells that had been transiently transfected with FLAG-tagged wild-type (WT, lane 1) or mutant SOD1 expression vector (lanes 2–6) were immunoprecipitated with anti-FLAG antibody (lanes 1–5) or normal IgG (lane 6). Immunoprecipitates were analyzed by immunoblotting specific for Hsp105 (top panel) or FLAG (second panel). The arrowhead and the asterisk indicate Hsp105 and non-specific bands, respectively. Ten micrograms (as protein) of each lysate that was subjected to immunoprecipitation were analyzed by immunoblotting (third and fourth panels). (b) Proteins in extracts of spinal cord and of liver from non-transgenic, $SOD^{WT}$, and $SOD^{G93A}$ mice were immunoprecipitated with anti-SOD1 antibody. Blots were probed for Hsp105 (top panel) or SOD1 (second panel). Eight micrograms (as protein) of the lysate used for immunoprecipitation were immunoblotted with indicated antibodies (third and fourth panels). The arrowhead and the asterisk indicate human SOD1 and endogenous mouse SOD1, respectively. (c) Confocal fluorescence micrographs of lumbar spinal cord from a non-transgenic mouse after double staining with SMI32 antibody (left panel) and anti-Hsp105 antibody (middle panel), and the merged image (right panel). Arrowheads indicate motor neurons that immunoreacted with both antibodies. Arrows indicate non-motor neurons that immunoreacted with only anti-Hsp105 antibody. Hsp105 was mainly localized in the cytoplasm of motor neurons. Scale bars: 50 μm.

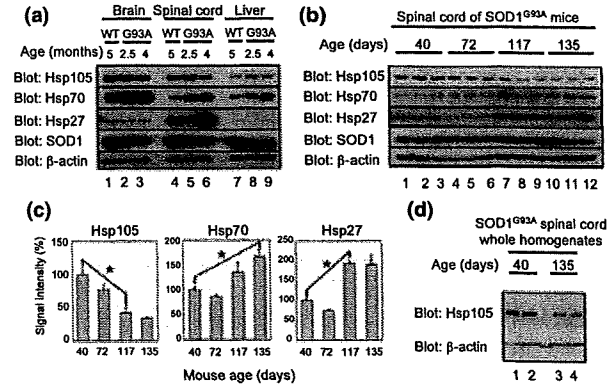


**Fig. 3** Decreases in the levels of expression of Hsp105 in the spinal cord during disease progression in superoxide dismutase 1 ($SOD1^{G93A}$) mice. (a) Immunoblotting analysis of Hsp105, Hsp70, and Hsp27 in the brain, spinal cord, and liver of $SOD1^{WT}$ and $SOD1^{G93A}$ mice at two different ages, as indicated. A total of 15 μg of protein was loaded in each lane. The level of Hsp105 was lower in the spinal cord of symptomatic $SOD1^{G93A}$ mice (4 months; lane 6) than in pre-symptomatic $SOD1^{G93A}$ mice (2.5 months; lane 5) (upper panel). The same membrane was immunoprobed for Hsp70 (second panel), Hsp27 (third panel), hSOD1 (fourth panel), and β-actin as a loading control (fifth panel). (b) Immunoblotting analysis of Hsp105, Hsp70, and Hsp27 in the spinal cord of early pre-symptomatic (40-day old), late pre-symptomatic (72-day old), symptomatic (117-day old), and end-stage (135-day old) $SOD1^{G93A}$ mice ($n = 3$ at each time point). A total of 15 μg of protein was loaded in each lane. Membranes were blotted with the indicated antibodies. (c) Densitometric analysis of the immunoblots shown in Fig. 3b. Results are expressed relative to the intensity of signals for 40-day-old mice, which were normalized to 100%. Values are expressed as means ± SE. Asterisks indicate significant difference ($p < 0.05$). (d) Immunoblotting analysis of Hsp105 using whole homogenates from the spinal cord of $SOD1^{G93A}$ mice at pre-symptomatic (40-day old) and end-stage (135-day old). A total of 40 μg of protein was loaded in each lane. Membranes were blotted with the indicated antibodies.

## Decreased expression of Hsp105 during disease progression in $SOD1^{G93A}$ mice

Heat-shock responses such as increased levels of Hsp27, Hsp70, and Hsp90 have been reported in the spinal cords of mutant SOD1 transgenic mice (Vleminckx *et al.* 2002; Liu *et al.* 2005). To examine changes in levels of heat-shock proteins, including Hsp105, we performed immunoblotting analyses of Hsp105, Hsp70, and Hsp27 in the brain, spinal cord, and liver of $SOD^{WT}$ mice at 5 months of age and in $SOD1^{G93A}$ mice at two different ages. By contrast to levels of other heat-shock proteins, the level of Hsp105 was lower in the spinal cord of symptomatic $SOD1^{G93A}$ mice (4-months old) than in that of pre-symptomatic $SOD1^{G93A}$ mice (2.5-months old) (Fig. 3a, upper panel, lanes 5 and 6).

To investigate the level of expression of heat-shock proteins in $SOD1^{G93A}$ mouse spinal cord in grater detail, we performed immunoblotting analysis of Hsp105, Hsp70, and Hsp27 in spinal cords from early pre-symptomatic (40-day old), late pre-symptomatic (72-day old), symptomatic (117-day old), and end-stage (135-day old) $SOD1^{G93A}$ mice (Fig. 3b). Decreased levels of Hsp105 were apparent as early as late pre-symptomatic stage (72 days). However, the decrease did not reach statistical significance. The expression of Hsp105 was significantly depressed as the disease progressed, whereas the levels of expression of both Hsp70 and Hsp27 were elevated at the symptomatic stage and the end-stage (Figs 3b and c). Semi-quantitative immunoblotting confirmed ≈50% decrease of level of Hsp105 in the spinal cord lysates from end-stage $SOD1^{G93A}$ mice (135-day old)

compared with ones from pre-symptomatic mice (40-day old) (Fig. S1).

To investigate whether the decrease in Hsp105 level was associated with the recruitment of Hsp105 to NP-40-insoluble fraction, we performed immunoblotting analysis using whole homogenates from the spinal cord of $SOD1^{G93A}$ mice at pre-symptomatic and end-stage. Whole homogenates were prepared by homogenizing mouse spinal cords with sample buffer for SDS–PAGE and analyzed by immunobloting. The significant decrease in Hsp105 level at end-stage was still observed (Fig. 3d), suggesting that the decrease of Hsp105 was unlikely to be due to the sequestration of Hsp105 into the insoluble fraction.

### Inhibition by Hsp105 of the formation of mutant SOD1-containing aggregates in cultured cells

Intracellular inclusions that are strongly immunopositive for SOD1 are found in the motor neurons of mutant SOD1 transgenic mice and in human ALS patients with a mutation in SOD1 (Bruijn *et al.* 1998). These misfolded, detergent-resistant protein aggregates are considered to be relevant to progression of the disease as increased accumulation of these aggregates has been observed in symptomatic mutant SOD1 mice (Bruijn *et al.* 1997; Johnston *et al.* 2000; Wang *et al.* 2002b). To determine whether Hsp105 can suppress the formation of mutant SOD1-containing aggregates, we studied the effects of over-expression of Hsp105 on the aggregation of mutant SOD1 in a filter trap assay. We co-transfected HEK293T cells with an $SOD1^{G93A}$-FLAG expression vector together with the empty vector, a vector that encoded β-galactosidase or a vector that encoded Hsp105. After 48 h, we harvested the cells and processed them for the filter trap assay. We examined the SDS-insoluble SOD1 aggregates that were retained on cellulose acetate membranes by immunoblotting. Hsp105 significantly suppressed the aggregation of mutant SOD1 (Fig. 4, upper panel). Moreover, the level of expression of $SOD1^{G93A}$ in HEK293T cells was very similar in all the samples examined. Taken together, the results indicate that Hsp105 reduced the level of mutant SOD1-containing aggregates by inhibiting the formation of aggregates rather than by facilitating their degradation.

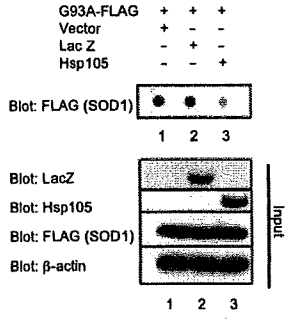


**Fig. 4** Hsp105 suppressed the aggregation of mutant superoxide dismutase 1 (SOD1) in cultured cells. HEK293T cells were co-transfected with an $SOD1^{G93A}$-FLAG expression vector together with the empty vector, an expression vector for β-galactosidase (LacZ), or an expression vector for Hsp105, as indicated. Lysates were analyzed by the filter trap assay with subsequent immunoblotting with anti-FLAG antibody, as described in the text (upper panel). The experiment was repeated three times with essentially the same results. Lower panels show the results of analysis of input in the filter trap assay.

## Discussion

In the present study, we have identified a novel interaction between Hsp105 and mutant SOD1 both in cultured cells and in a mouse model. Although the involvement of other heat-shock proteins has been demonstrated in mutant SOD1-mediated toxicity, we demonstrated, for the first time to our knowledge, a decrease in the level of expression of Hsp105, specifically, from the symptomatic to the end-stage of disease in the mutant SOD1 mouse model unlike other heat-shock proteins (Fig. 3). This result might be explained by several properties of Hsp105, which make it uniquely different from Hsp70, a major molecular chaperone that is involved in the folding of newly synthesized and misfolded proteins, even though these heat-shock proteins are structurally similar.

Hsp105, which is a constitutively expressed 105-kDa protein whose synthesis is enhanced by the various stress stimuli, is concentrated in the brain, which suggests a specific role for Hsp105 in stress responses within the nervous system (Lee-Yoon *et al.* 1995; Yasuda *et al.* 1995). Hsp105 exhibits significant homology at the amino acid level to Hsp70, in particular in the amino-terminal ATPase domain. The chaperone activity of Hsp70/Hsc70 (Hsp70s) is controlled by a series of ATP-dependent reaction cycles that consist of the binding of ATP, hydrolysis of ATP, and nucleotide exchange (Buchberger *et al.* 1995; McCarty *et al.* 1995; Rudiger *et al.* 1997). By contrast, Hsp105 does not require ATP to prevent the aggregation of denatured proteins (Yamagishi *et al.* 2003), but it does act as a nucleotide-exchange factor for Hsp70s, which suggests a role for Hsp105 in supporting the functions of Hsp70s (Dragovic *et al.* 2006; Raviol *et al.* 2006). Hsp105 binds to denatured proteins *in vitro* and maintains these proteins in a folding-competent state rather than refolding them itself (Oh *et al.* 1997, 1999; Yamagishi *et al.* 2003). Thus, Hsp105 might function not only in collaboration with Hsp70s but also as a substitute for Hsp70s under severe stress condition, when cellular supplies of ATP have been markedly depleted. In motor neurons that express mutant SOD1, Hsp70s might not be functional, since the level of cellular ATP is likely to be low as a result of consumption by Hsp70s and the ubiquitin-proteasome system. This scenario might explain the failure of over-expression of Hsp70 to mitigate the toxicity of mutant SOD1 in mice (Liu *et al.* 2005). Therefore, rather than

 

Hsp70, Hsp105 might be a promising candidate for a suppressor of mutant SOD1 toxicity.

We observed the decreased level of Hsp105 in spinal cord of $SOD1^{G93A}$ mice as disease progressed (Fig. 3b) and further confirmed ≈50% decrease in Hsp105 levels at end-stage by semi-quantitative immunoblotting analysis (Fig. S1). This result might partly reflect the loss of motor neurons, which contain abundant Hsp105 proteins. However, considering the facts that lumbar spinal cord sections of $SOD1^{G93A}$ mice at the end-stage show approximately 50% loss of motor neurons (Kostic *et al.* 1997; Bendotti and Carri 2004) and that Hsp105 is expressed not only in motor neurons but also in non-motor neurons (Fig. 2c), it is less likely that Hsp105 was decreased as a consequence of only motor neuronal loss. Immunoblotting analysis of whole spinal cord homogenates also revealed the decreased level of Hsp105 in spinal cord of $SOD1^{G93A}$ mice (Fig. 3d). Therefore, although a fraction of Hsp105 might be lost in aggregates, a significant part of Hsp105 is likely to be consumed or degraded by interacting with mutant SOD1.

Consistent with the reports of the ability of Hsp105 to maintain denatured proteins in a folding-competent state (Oh *et al.* 1997, 1999; Yamagishi *et al.* 2003), we have shown that Hsp105 is able to suppress the formation of aggregates of mutant SOD1 in cultured cells. Mutant SOD1-containing aggregates immunoreact strongly with antibodies raised against ubiquitin, and this phenomenon is common to all mutant SOD1-expressing mouse models (Bruijn *et al.* 1998; Wang *et al.* 2003; Jonsson *et al.* 2004) and human patients (Bruijn *et al.* 1998; Kato *et al.* 2000; Watanabe *et al.* 2001). These findings, together with decreased expression of Hsp105 in symptomatic $SOD1^{G93A}$ mice, suggest that depletion of Hsp105 might contribute to the process of motor neuron degeneration through the accumulation of aggregates of misfolded mutant SOD1.

Hsp105 is essential for cell survival in eukaryotes. Combined deletion in yeast cells of the *SSE1* and *SSE2* genes, which encode members of the Hsp105/110 family, is lethal (Raviol *et al.* 2006). Moreover, recessive mutations in the *SIL1* gene, whose product functions as a nucleotide-exchange factor for the protein of the Hsp70 family, Bip (GRP78), are responsible for Marinesco–Sjögren syndrome, which is characterized by cerebellar atrophy with degeneration of Purkinje and granule cells (Anttonen *et al.* 2005; Senderek *et al.* 2005). Combined with recent reports that Hsp105 is a nucleotide-exchange factor for Hsp70s, these findings provide a link between a functional deficit in a nucleotide-exchange factor for the proteins of the Hsp70 family and neurodegeneration. With respect to neuronal survival, over-expression of Hsp105 has an anti-apoptotic effect in cultured neuronal PC12 cells (Hatayama *et al.* 2001). Hsp105 suppresses apoptosis in a cell culture model of polyglutamine disease, a neurodegenerative disease caused by the toxicity that is derived from a misfolded mutant protein (Ishihara *et al.* 2003). Moreover, we observed Hsp105 prevented caspase-activation induced by proteasomal inhibition with lactacystin in neuroblastoma cell line (Yamashita *et al.*, unpublished data). These results suggest that enhanced expression of Hsp105 might contribute to prevention of motor neuron degeneration through its anti-apoptotic property.

Increased expression of Hsp70s in spinal cord lysates from our $SOD1^{G93A}$ mice and from $SOD1^{G85R}$ mice (Liu *et al.* 2005), together with the impaired heat-shock response of Hsp70 in mutant SOD1-expressing motor neurons (Batulan *et al.* 2003), suggests the enhanced expression of Hsp70s in glial cells. In accordance with this hypothesis, elevated levels of Hsp27 were also observed in the glial cells of $SOD1^{G93A}$ mice (Vleminckx *et al.* 2002). However, this scenario does not apply to Hsp105, because (i) continuous decreases in levels of Hsp105 were observed throughout the course of the disease and (ii) Hsp105 is concentrated in neurons and not in glial cells (Hylander *et al.* 2000). Absence of the induction of expression of Hsp105 in non-neuronal glial cells might exacerbate the toxicity of mutant SOD1 as the toxicity of the mutant protein to motor neurons is non-cell autonomous (Clement *et al.* 2003; Boillee *et al.* 2006).

Over-expression of Hsp70 did not ameliorate the condition of mutant SOD1 mice (Liu *et al.* 2005). By contrast, the pharmacological activation of HSF-1, a transcription factor for heat-shock proteins, extended the life span of mutant SOD1 mice by enhancing the expression of Hsp70s and Hsp90. In the cited study, the level of Hsp105 was not measured (Kieran *et al.* 2004). In spinal and bulbar muscular atrophy mouse model, in which accumulation of misfolded polyglutamine protein causes motor neuron degeneration, pharmacological induction of the expression of HSF-1 by geranylgeranylacetone alleviated polyglutamine-mediated motor neuron disease and activation of HSF-1 was shown to induce the expression of Hsp70, Hsp90, and Hsp105 but not of Hsp27, Hsp40, and Hsp60 (Katsuno *et al.* 2005). In view of our observation of depleted supplies of Hsp105 in $SOD1^{G93A}$ mice, a requirement for enhanced synthesis of Hsp70s, Hsp90, and Hsp105 in both neuronal cells and non-neuronal neighboring cells might be crucial for the mitigation of mutant SOD1-mediated toxicity.

## Acknowledgements

The authors thank Dr K. Ishihara (RIKEN Brain Science Institute) for a critical review of the original manuscript, Ms K. Odan (Kyoto University) for technical assistance, and Drs K. Uemura and A. Kuzuya (Kyoto University) for kind advice. This work was supported by the Nakabayashi Trust for ALS Research; the Ministry of Education, Culture, Sports, Science and Technology of Japan; the Ministry of Health, Labor and Welfare of Japan; the Smoking Research Foundation; Philip Morris USA Inc. and Philip Morris International.

 

## Supplementary material

The following supplementary material is available for this article online:

**Fig. S1** Semi-quantitative analysis of Hsp105 levels in the spinal cord of SOD1G93A mice.

This material is available as part of the online article from http://www.blackwell-synergy.com.

## References


Andersen P. M., Forsgren L., Binzer M. *et al.* (1996) Autosomal recessive adult-onset amyotrophic lateral sclerosis associated with homozygosity for Asp90Ala CuZn-superoxide dismutase mutation. A clinical and genealogical study of 36 patients. *Brain* **119**(Pt. 4), 1153–1172.

Anttonen A. K., Mahjneh I., Hamalainen R. H. *et al.* (2005) The gene disrupted in Marinesco-Sjogren syndrome encodes SIL1, an HSPA5 cochaperone. *Nat. Genet.* **37**, 1309–1311.

Batulan Z., Shinder G. A., Minotti S., He B. P., Doroudchi M. M., Nalbantoglu J., Strong M. J. and Durham H. D. (2003) High threshold for induction of the stress response in motor neurons is associated with failure to activate HSF1. *J. Neurosci.* **23**, 5789–5798.

Bendotti C. and Carri M. T. (2004) Lessons from models of SOD1-linked familial ALS. *Trends Mol. Med.* **10**, 393–400.

Boillee S., Yamanaka K., Lobsiger C. S., Copeland N. G., Jenkins N. A., Kassiotis G., Kollias G. and Cleveland D. W. (2006) Onset and progression in inherited ALS determined by motor neurons and microglia. *Science* **312**, 1389–1392.

Bruening W., Roy J., Giasson B., Figlewicz D. A., Mushynski W. E. and Durham H. D. (1999) Up-regulation of protein chaperones preserves viability of cells expressing toxic Cu/Zn-superoxide dismutase mutants associated with amyotrophic lateral sclerosis. *J. Neurochem.* **72**, 693–699.

Bruijn L. I., Becher M. W., Lee M. K. *et al.* (1997) ALS-linked SOD1 mutant G85R mediates damage to astrocytes and promotes rapidly progressive disease with SOD1-containing inclusions. *Neuron* **18**, 327–338.

Bruijn L. I., Houseweart M. K., Kato S., Anderson K. L., Anderson S. D., Ohama E., Reaume A. G., Scott R. W. and Cleveland D. W. (1998) Aggregation and motor neuron toxicity of an ALS-linked SOD1 mutant independent from wild-type SOD1. *Science* **281**, 1851–1854.

Bruijn L. I., Miller T. M. and Cleveland D. W. (2004) Unraveling the mechanisms involved in motor neuron degeneration in ALS. *Annu. Rev. Neurosci.* **27**, 723–749.

Buchberger A., Theyssen H., Schroder H., McCarty J. S., Virgallita G., Milkereit P., Reinstein J. and Bukau B. (1995) Nucleotide-induced conformational changes in the ATPase and substrate binding domains of the DnaK chaperone provide evidence for interdomain communication. *J. Biol. Chem.* **270**, 16 903–16 910.

Choi J. S., Cho S., Park S. G., Park B. C. and Lee D. H. (2004) Co-chaperone CHIP associates with mutant Cu/Zn-superoxide dismutase proteins linked to familial amyotrophic lateral sclerosis and promotes their degradation by proteasomes. *Biochem. Biophys. Res. Commun.* **321**, 574–583.

Clement A. M., Nguyen M. D., Roberts E. A. *et al.* (2003) Wild-type nonneuronal cells extend survival of SOD1 mutant motor neurons in ALS mice. *Science* **302**, 113–117.

Dragovic Z., Broadley S. A., Shomura Y., Bracher A. and Hartl F. U. (2006) Molecular chaperones of the Hsp110 family act as nucleotide exchange factors of Hsp70s. *EMBO J.* **25**, 2519–2528.

Hand C. K., Mayeux-Portas V., Khoris J., Briolotti V., Clavelou P., Camu W. and Rouleau G. A. (2001) Compound heterozygous D90A and D96N SOD1 mutations in a recessive amyotrophic lateral sclerosis family. *Ann. Neurol.* **49**, 267–271.

Hatayama T., Yamagishi N., Minobe E. and Sakai K. (2001) Role of hsp105 in protection against stress-induced apoptosis in neuronal PC12 cells. *Biochem. Biophys. Res. Commun.* **288**, 528–534.

Hylander B. L., Chen X., Graf P. C. and Subjeck J. R. (2000) The distribution and localization of hsp110 in brain. *Brain Res.* **869**, 49–55.

Ishihara K., Yamagishi N., Saito Y., Adachi H., Kobayashi Y., Sobue G., Ohtsuka K. and Hatayama T. (2003) Hsp105alpha suppresses the aggregation of truncated androgen receptor with expanded CAG repeats and cell toxicity. *J. Biol. Chem.* **278**, 25 143–25 150.

Jensen O. N., Podtelejnikov A. and Mann M. (1996) Delayed extraction improves specificity in database searches by matrix-assisted laser desorption/ionization peptide maps. *Rapid Commun. Mass Spectrom.* **10**, 1371–1378.

Johnston J. A., Dalton M. J., Gurney M. E. and Kopito R. R. (2000) Formation of high molecular weight complexes of mutant Cu, Zn-superoxide dismutase in a mouse model for familial amyotrophic lateral sclerosis. *Proc. Natl Acad. Sci. USA* **97**, 12 571–12 576.

Jonsson P. A., Ernhill K., Andersen P. M., Bergemalm D., Brannstrom T., Gredal O., Nilsson P. and Marklund S. L. (2004) Minute quantities of misfolded mutant superoxide dismutase-1 cause amyotrophic lateral sclerosis. *Brain* **127**, 73–88.

Kato S., Takikawa M., Nakashima K., Hirano A., Cleveland D. W., Kusaka H., Shibata N., Kato M., Nakano I. and Ohama E. (2000) New consensus research on neuropathological aspects of familial amyotrophic lateral sclerosis with superoxide dismutase 1 (SOD1) gene mutations: inclusions containing SOD1 in neurons and astrocytes. *Amyotroph. Lateral Scler. Other Motor Neuron Disord.* **1**, 163–184.

Katsuno M., Sang C., Adachi H., Minamiyama M., Waza M., Tanaka F., Doyu M. and Sobue G. (2005) Pharmacological induction of heat-shock proteins alleviates polyglutamine-mediated motor neuron disease. *Proc. Natl Acad. Sci. USA* **102**, 16 801–16 806.

Kieran D., Kalmar B., Dick J. R., Riddoch-Contreras J., Burnstock G. and Greensmith L. (2004) Treatment with arimoclomol, a coinducer of heat shock proteins, delays disease progression in ALS mice. *Nat. Med.* **10**, 402–405.

Kostic V., Gurney M. E., Deng H. X., Siddique T., Epstein C. J. and Przedborski S. (1997) Midbrain dopaminergic neuronal degeneration in a transgenic mouse model of familial amyotrophic lateral sclerosis. *Ann. Neurol.* **41**, 497–504.

Lee-Yoon D., Easton D., Murawski M., Burd R. and Subjeck J. R. (1995) Identification of a major subfamily of large hsp70-like proteins through the cloning of the mammalian 110-kDa heat shock protein. *J. Biol. Chem.* **270**, 15 725–15 733.

Liu J., Shinobu L. A., Ward C. M., Young D. and Cleveland D. W. (2005) Elevation of the Hsp70 chaperone does not effect toxicity in mouse models of familial amyotrophic lateral sclerosis. *J. Neurochem.* **93**, 875–882.

Maatkamp A., Vlug A., Haasdijk E., Troost D., French P. J. and Jaarsma D. (2004) Decrease of Hsp25 protein expression precedes degeneration of motoneurons in ALS-SOD1 mice. *Eur. J. Neurosci.* **20**, 14–28.

McCarty J. S., Buchberger A., Reinstein J. and Bukau B. (1995) The role of ATP in the functional cycle of the DnaK chaperone system. *J. Mol. Biol.* **249**, 126–137.

Miyazaki K., Fujita T., Ozaki T. *et al.* (2004) NEDL1, a novel ubiquitin-protein isopeptide ligase for dishevelled-1, targets mutant superoxide dismutase-1. *J. Biol. Chem.* **279**, 11 327–11 335.

Niwa J., Ishigaki S., Hishikawa N., Yamamoto M., Doyu M., Murata S., Tanaka K., Taniguchi N. and Sobue G. (2002) Dorfin ubiquitylates mutant SOD1 and prevents mutant SOD1-mediated neurotoxicity. *J. Biol. Chem.* **277**, 36 793–36 798.


 

Oeda T., Shimohama S., Kitagawa N., Kohno R., Imura T., Shibasaki H. and Ishii N. (2001) Oxidative stress causes abnormal accumulation of familial amyotrophic lateral sclerosis-related mutant SOD1 in transgenic Caenorhabditis elegans. *Hum. Mol. Genet.* **10**, 2013–2023.

Oh H. J., Chen X. and Subjeck J. R. (1997) Hsp110 protects heat-denatured proteins and confers cellular thermoresistance. *J. Biol. Chem.* **272**, 31 636–31 640.

Oh H. J., Easton D., Murawski M., Kaneko Y. and Subjeck J. R. (1999) The chaperoning activity of hsp110. Identification of functional domains by use of targeted deletions. *J. Biol. Chem.* **274**, 15 712–15 718.

Okado-Matsumoto A. and Fridovich I. (2002) Amyotrophic lateral sclerosis: a proposed mechanism. *Proc. Natl Acad. Sci. USA* **99**, 9010–9014.

Parton M. J., Andersen P. M., Broom W. J. and Shaw C. E. (2001) Compound heterozygosity and variable penetrance in SOD1 amyotrophic lateral sclerosis pedigrees. *Ann. Neurol.* **50**, 553–554.

Raviol H., Sadlish H., Rodriguez F., Mayer M. P. and Bukau B. (2006) Chaperone network in the yeast cytosol: Hsp110 is revealed as an Hsp70 nucleotide exchange factor. *EMBO J.* **25**, 2510–2518.

Rudiger S., Buchberger A. and Bukau B. (1997) Interaction of Hsp70 chaperones with substrates. *Nat. Struct. Biol.* **4**, 342–349.

Senderek J., Krieger M., Stendel C. *et al.* (2005) Mutations in SIL1 cause Marinesco-Sjogren syndrome, a cerebellar ataxia with cataract and myopathy. *Nat. Genet.* **37**, 1312–1314.

Shinder G. A., Lacourse M. C., Minotti S. and Durham H. D. (2001) Mutant Cu/Zn-superoxide dismutase proteins have altered solubility and interact with heat shock/stress proteins in models of amyotrophic lateral sclerosis. *J. Biol. Chem.* **276**, 12 791–12 796.

Urushitani M., Kurisu J., Tateno M., Hatakeyama S., Nakayama K., Kato S. and Takahashi R. (2004) CHIP promotes proteasomal degradation of familial ALS-linked mutant SOD1 by ubiquitinating Hsp/Hsc70. *J. Neurochem.* **90**, 231–244.

Vleminckx V., Van Damme P., Goffin K., Delye H., Van Den Bosch L. and Robberecht W. (2002) Upregulation of HSP27 in a transgenic model of ALS. *J. Neuropathol. Exp. Neurol.* **61**, 968–974.

Wang J., Xu G. and Borchelt D. R. (2002a) High molecular weight complexes of mutant superoxide dismutase 1: age-dependent and tissue-specific accumulation. *Neurobiol. Dis.* **9**, 139–148.

Wang J., Xu G., Gonzales V., Coonfield M., Fromholt D., Copeland N. G., Jenkins N. A. and Borchelt D. R. (2002b) Fibrillar inclusions and motor neuron degeneration in transgenic mice expressing superoxide dismutase 1 with a disrupted copper-binding site. *Neurobiol. Dis.* **10**, 128–138.

Wang J., Slunt H., Gonzales V., Fromholt D., Coonfield M., Copeland N. G., Jenkins N. A. and Borchelt D. R. (2003) Copper-binding-site-null SOD1 causes ALS in transgenic mice: aggregates of non-native SOD1 delineate a common feature. *Hum. Mol. Genet.* **12**, 2753–2764.

Watanabe M., Dykes-Hoberg M., Culotta V. C., Price D. L., Wong P. C. and Rothstein J. D. (2001) Histological evidence of protein aggregation in mutant SOD1 transgenic mice and in amyotrophic lateral sclerosis neural tissues. *Neurobiol. Dis.* **8**, 933–941.

Yamagishi N., Ishihara K., Saito Y. and Hatayama T. (2003) Hsp105 but not Hsp70 family proteins suppress the aggregation of heat-denatured protein in the presence of ADP. *FEBS Lett.* **555**, 390–396.

Yasuda K., Nakai A., Hatayama T. and Nagata K. (1995) Cloning and expression of murine high molecular mass heat shock proteins, HSP105. *J. Biol. Chem.* **270**, 29 718–29 723.

 

# PINK1, a gene product of PARK6, accumulates in α-synucleinopathy brains

Tetsuro Murakami, Yasuhiro Moriwaki, Takeshi Kawarabayashi, et al.

*J Neurol Neurosurg Psychiatry* 2007 78: 653-654 originally published online January 8, 2007
doi: 10.1136/jnnp.2006.100123

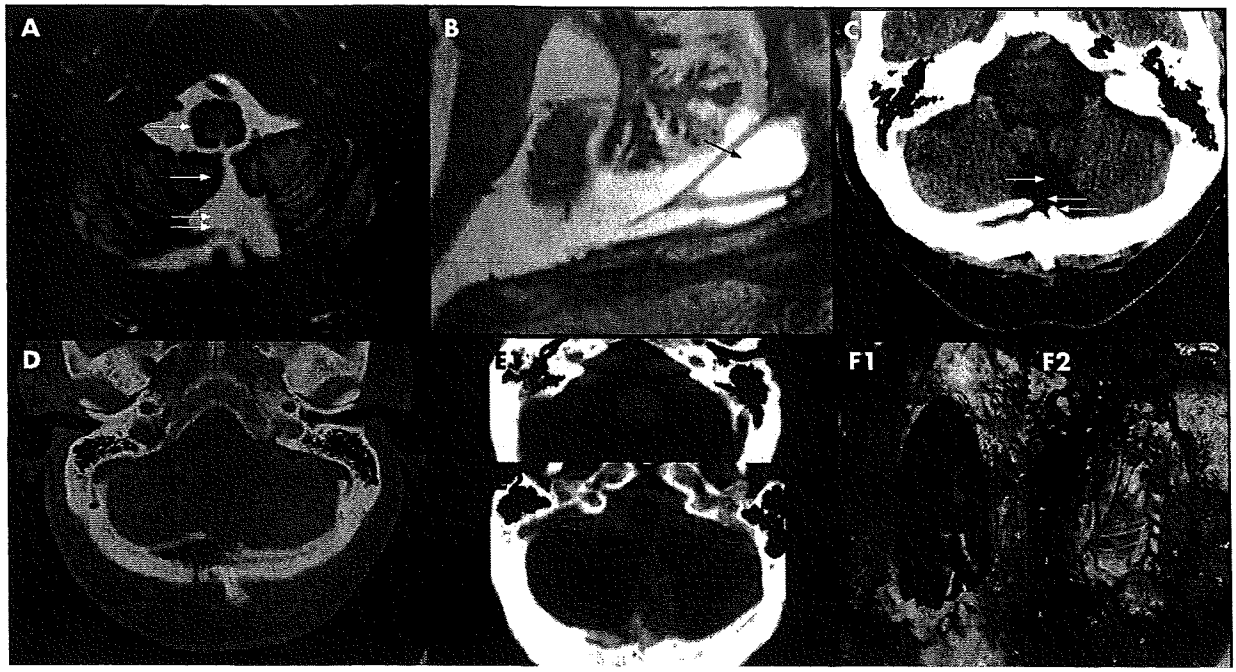


**Figure 1** A T2 weighted axial head MRI shows haemosiderin deposition along the cerebellar folia and around the brain stem (single arrows). Also shown is the posteriorly located cystic structure (double arrows). (B) T2 weighted sagittal head MRI shows the posteriorly located cystic structure. (C) Axial head CT showing the cystic structure (single arrow) and fracture of the inner table (double arrow). (D) Axial head CT (bony window) showing the discontinuity in the inner skull table. (E1, E2) CT myelogram showing extravasation of contrast from the fourth ventricle (E1) into the cystic structure (E2). (F1) Dural defect noted at the time of the suboccipital craniotomy. This was leading to the cyst through the defect in the inner table and was overlying the fourth ventricle from which CSF was flowing into the cyst. (F2) Site after repair of dural defect.

likely bleeding source. It is speculative whether exposure of CSF to extradural tissue may lead to SS by an unidentified mechanism. Given the long natural history of SS, the available follow-up duration of 3 months is too brief to assess response to the intervention. Intradiploic CSF fistulas are exceedingly rare.[8] They are generally benign and are often related to trauma or neurosurgical procedures. No case with associated SS has been reported.

**Neeraj Kumar**
Department of Neurology, Mayo Clinic, Rochester, Minnesota, USA

**Jonathan M Bledsoe, Dudley H Davis**
Department of Neurosurgery, Mayo Clinic, Rochester, Minnesota, USA

Correspondence to: Dr Neeraj Kumar, Department of Neurology, Mayo Clinic, 200 First Street SW, Rochester, MN 55905, USA; kumar.neeraj@mayo.edu

doi: 10.1136/jnnp.2006.108225

**Published Online First 18 December 2006**

Competing interests: None.

## References

1 **Borke RC**, Stevens I. Superficial siderosis of the central nervous system. A 37-year follow-up of a case and review of the literature. *J Neuropathol Exp Neurol* 1991;**50**:579–94.
2 **Fearnley JM**, Stevens JM, Rudge P. Superficial siderosis of the central nervous system. *Brain* 1995;**118**:1051–66.
3 **Kumar N**, Cohen-Gadol AA, Wright RA, *et al*. Superficial siderosis. *Neurology* 2006;**66**:1144–52.
4 **Kumar N**. Superficial siderosis: Associations and therapeutic implications. *Arch Neurol* 2007. In press.
5 **Wilden JA**, Kumar N, Murali HR, *et al*. Unusual neuroimaging in superficial siderosis. *Neurology* 2005;**65**:489.
6 **Kumar N**, Lindell EP, Wilden JA, *et al*. Role of dynamic CT myelography in identifying the etiology of superficial siderosis. *Neurology* 2005;**65**:486–8.
7 **Bürk K**, Skaley M, Dichgans J. High prevalence of CSF-containing cysts in superficial hemosiderosis of the central nervous system. *J Neurol* 2001;**248**:1005–6.
8 **Placantonakis DG**, Lis E, Souweidane MM. Intradiploic cerebrospinal fluid fistulas of iatrogenic origin. *J Neurosurg* 2006;**104**:356–9.

## PINK1, a gene product of PARK6, accumulates in α-synucleinopathy brains

α-Synucleinopathy is an entity of neurodegenerative diseases such as Parkinson's disease (PD), dementia with Lewy bodies (DLB) and multiple system atrophy (MSA), that involves accumulation of α-synuclein in the brain. PINK1 (PTEN induced kinase 1) is a novel gene recently identified as causative in autosomal recessive early onset parkinsonism (PARK6). In the present study, we examined the localisation of PINK1 in the brains of patients with α-synucleinopathy and found PINK1 in glial cytoplasmic inclusions (GCIs) in MSA, as well as in Lewy bodies (LBs) in PD and DLB. These findings imply that PINK1 may be involved in the formation of LBs and GCIs, suggesting that PINK1 is one of the major pathological proteins in α-synucleinopathy.

### Methods

The cDNA of PINK1, corresponding to 112–520 amino acids of the protein, was subcloned in a vector pET30(a) with a His tag. Anti-PINK1 antibody was generated against recombinant His tagged PINK1 by immunising a rabbit. The obtained antibody was affinity purified. A postmortem brain sample from a normal patient was homogenised, subjected to sodium dodecyl sulphate-polyacrylamide gel electrophoresis and transferred to a membrane. After blocking in Tris buffered saline with 5% dry milk, the membrane was incubated with anti-PINK1 antibody (1:1000). The membrane was then incubated with a secondary antibody (1:2500; Amersham, Buckinghamshire, UK), and visualised with an enhanced chemiluminescent substrate (Pierce, Rockford, Illinois, USA). Immunohistochemical analysis was carried out with paraffin embedded midbrain sections from patients with sporadic PD, DLB and MSA, and from normal controls (n = 6, 3, 6 and 6, respectively). First, localisation of PINK1 protein in normal human brain was examined by carrying out double staining of PINK1 (1:500) and cytochrome c (1:1000, mouse monoclonal; Pharmingen, Germany). Sections from patients with PD, DLB and MSA, and from normal controls were immunostained with anti-PINK1 antibody as previously described.[1]

### Results

Immunoblotting analysis revealed that the anti-PINK1 antibody detected a major band of approximately 50 kDa, corresponding to mature PINK1 protein (PINK1 without a

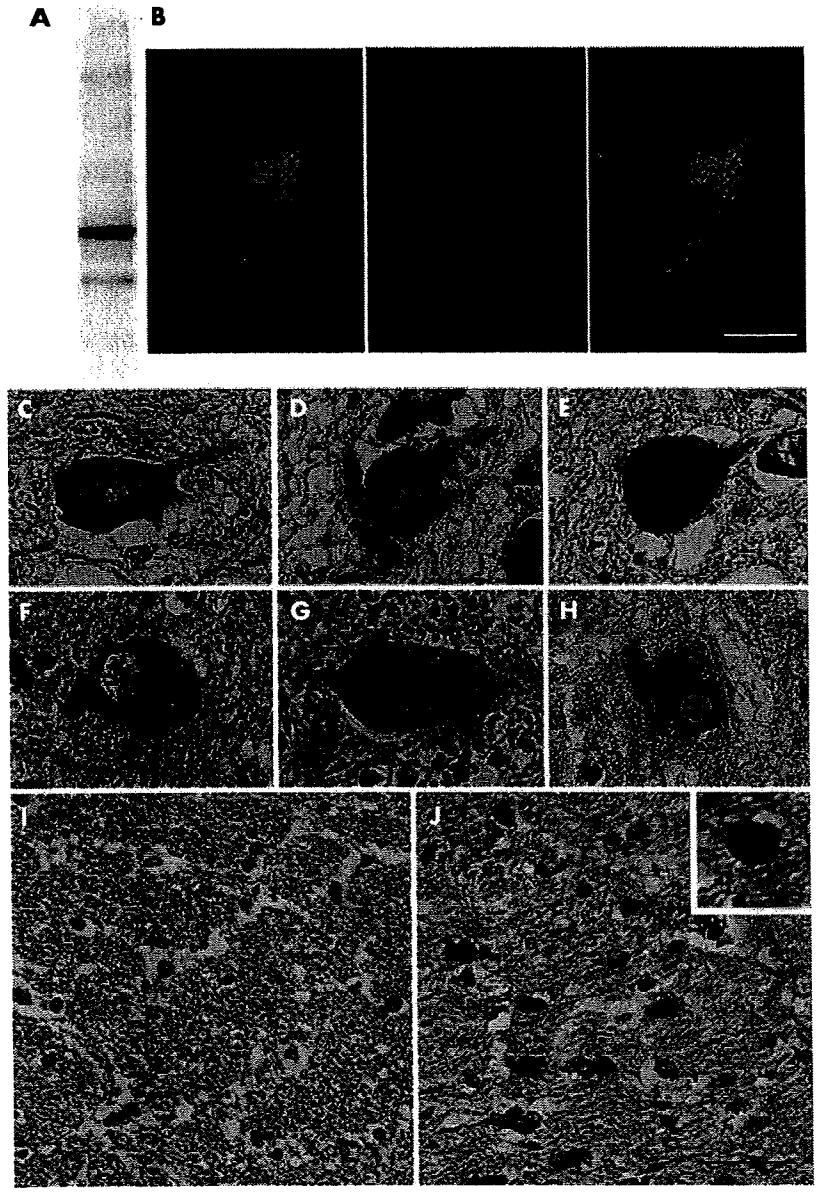


**Figure 1** Immunoblotting of a normal human brain (non-fractionated sample) with anti-PTEN induced kinase 1 (PINK1) antibody (A). The antibody mainly detected a band at a molecular weight of 50 kDa, which corresponds to the mature form of PINK1. (B) Double immunofluorescent staining of PINK1 and cytochrome c in the substantia nigra of a normal control brain. Note that PINK1 and cytochrome c colocalised well. Scale bar is 50 μm. Immunohistochemical analyses of PINK1 in a normal human control (C, I) and in the brains of patients with α-synucleinopathy (D–H, J). In the normal control, substantial PINK1 immunoreactivity was detected in the cytoplasm of the substantia nigra (A). In Parkinson's disease, PINK1 mostly accumulated in the halo of Lewy bodies (LBs) (D–H). Some LBs were stained in the core (H). In the crus cerebri of the normal control, no immunostaining was observed (I), whereas in patients with multiple system atrophy, extensive and diffuse staining was seen in almost all glial cytoplasmic inclusions (J, insert). Scale bar is 50 μm in B–J and 10 μm in J (insert).

mitochondrial targeting signal), and a weak additional band at 40 kDa (fig 1A). An absorption experiment revealed that the antibody specifically recognised PINK1 protein. Double staining of PINK1 and cytochrome c showed dot-like stainings in the cytoplasm (fig 1B). PINK1 and cytochrome c were colocalised, suggesting that PINK1 is localised to the mitochondria. In the immunohistochemical analysis, dot-like staining of PINK1 was observed in the cytoplasm of the substantia nigra of a normal control (fig 1C). In patients with PD and DLB, the majority of LBs were detected by the antibody. In most LBs, PINK1 was localised more intensely in the halo (fig 1D–G) whereas the core was more intensely stained in some LBs (fig 1H). In the crus cerebri of the normal control, no immunostaining was detected (fig 1I); however, in MSA brains, immunostaining demonstrated extensive distribution of immunoreactive GCIs (fig 1J). Almost all GCIs were detected by the antibody and stained diffusely in the cytoplasm (fig 1J, insert). For negative controls, some slides underwent the same procedure without the primary antibody and showed no staining (data not shown).

## Discussion

Immunoblotting analysis revealed that anti-PINK1 antibody mainly recognised the mature form of PINK1 (fig 1A). It also seems that normal neurons express substantial amounts of PINK1 at baseline (fig 1A–C). In the present study, we showed that PINK1 is a novel component of LBs and Lewy neuritis, suggesting that PINK1 is involved in LB formation in PD and DLB. We previously suggested that LBs are formed because of the disposal process of aberrant proteins, which otherwise could be cytotoxic.[1 2] The present study suggests that PINK1 might be involved in the pathway. PINK1 is a putative mitochondrial kinase, and may be associated with the phosphorylation of proteins.[3] The mechanism by which PINK1 is related with LB formation is unclear. One possibility is that PINK1 becomes unfolded and insoluble. Such PINK1 protein might accumulate in the inclusions. Another possibility is that PINK1 acquires activity changes. As a result, some substrates of PINK1 might also be altered and accumulate in LBs. Most cases of PARK6 are recessive, caused by homozygous PINK1 gene mutation, and loss of its function has been argued. Therefore, the latter hypothesis is more likely. Why PINK1, a predicted mitochondrial protein, accumulates in cytoplasmic inclusions needs to be addressed. Although the reason is unclear, several studies have revealed mitochondrial dysfunction in PD, and it may be involved in the participation of PINK1 in LB formation.

It should also be noted that PINK1 is detected in GCIs of brains from patients with MSA. To date, several molecules have been suggested to be associated, genetically or experimentally, with α-synucleinopathy, including the following: α-synuclein, Parkin, synphilin-1 and Pael-R. Among these molecules, only α-synuclein and synphilin-1 have been shown to be present in both LBs and GCIs.[4] PINK1 is the third molecule whose accumulation in these inclusions was confirmed. In anther study, however, it was reported that cortical LBs and GCIs are PINK1 negative.[5] The antibody used in the study by Gandhi *et al* does not recognise 50 kDa PINK1 in the insoluble fraction whereas our antibody detected only 50 kDa PINK1 in the whole fraction. Therefore, it is possible that the different solubility of PINK1 protein influenced the discrepancy; that is, if PINK1 in GCIs is still soluble, our antibody may be more sensitive to the protein in GCIs. The present result supports the possibility that PINK1 is involved in the common pathway of α-synucleinopathy, an entity of a neurodegenerative disorder, sharing a common cascade arising from the accumulation of α-synuclein to inclusion formation and cell death. Further proteomic investigations may clarify the normal and aberrant roles of PINK1 protein and, ideally, the mechanism of inclusion formation and therapeutics of α-synucleinopathy.

## Acknowledgements

This work was partly supported by Grants-in-Aid for Scientific Research (B) 16390251, 15390273, 17659445 and 18890112, and the National Project on Protein Structural and Functional Analyses from the Ministry of Education, Science, Culture and Sports of Japan, and by grants (Itoyama Y, Kimura Y, and Kuzuhara S) from the Ministry of Health and Welfare of Japan.

**Tetsuro Murakami**
Department of Neurology, Okayama University Graduate School of Medicine, Dentistry and Pharmaceutical Sciences, Okayama, Japan

**Yasuhiro Moriwaki**
Kyoritsu University of Pharmacy, Department of Clinical Pharmacy, Division of Pharmacology, Tokyo, Japan

**Takeshi Kawarabayashi, Makiko Nagai, Yasuyuki Ohta, Kentaro Deguchi, Tomoko Kurata, Nobutoshi Morimoto, Yasushi Takehisa**
Department of Neurology, Okayama University Graduate School of Medicine, Dentistry and Pharmaceutical Sciences, Okayama, Japan

**Etsuro Matsubara**
Department of Alzheimer's Disease Research, National Institute of Longevity Sciences, National Center for Geriatrics and Gerontology, Aichi, Japan

**Masaki Ikeda**
Department of Neurology, Gunma University Graduate School of Medicine, Gunma, Japan

**Yasuo Harigaya**
Department of Neurology, Maebashi Red Cross Hospital, Gunma, Japan

**Mikio Shoji**
Department of Neurology, Okayama University Graduate School of Medicine, Dentistry and Pharmaceutical Sciences, Okayama, Japan, and Department of Neurological Science, Institute of Brain Science, Hirosaki University School of Medicine, Aomori, Japan

**Ryosuke Takahashi**
Department of Neurology, Kyoto University Graduate School of Medicine, Kyoto, Japan

**Koji Abe**
Department of Neurology, Okayama University Graduate School of Medicine, Dentistry and Pharmaceutical Sciences, Okayama, Japan

Correspondence to: Tetsuro Murakami, Department of Neurology, Okayama University Graduate School of Medicine, Dentistry and Pharmaceutical Sciences, 2-5-1 Shikata-cho, Okayama 700-8558, Japan; neuron@cc.okayama-u.ac.jp

doi: 10.1136/jnnp.2006.100123

Competing interests: None.

## References

1 **Murakami T**, Shoji M, Imai Y, *et al*. Pael-R is accumulated in Lewy bodies of Parkinson's disease. *Ann Neurol* 2004;**55**:439–42.
2 **Imai Y**, Soda M, Inoue H, *et al*. An unfolded putative transmembrane polypeptide, which can lead to endoplasmic reticulum stress, is a substrate of Parkin. *Cell* 2001;**105**:891–902.
3 **Valente EM**, Abou-Sleiman PM, Caputo V, *et al*. Hereditary early-onset Parkinson's disease caused by mutations in PINK1. *Science* 2004;**304**:1158–60.
4 **Baba M**, Nakajo S, Tu PH, *et al*. Aggregation of alpha-synuclein in Lewy bodies of sporadic Parkinson's disease and dementia with Lewy bodies. *Am J Pathol* 1998;**152**:879–84.
5 **Gandhi S**, Muqit MM, Stanyer L, *et al*. PINK1 protein in normal human brain and Parkinson's disease. *Brain* 2006;**129**:1720–31.

## Diffusion tensor tracking of fornix infarction

Focal damage to the fornices is uncommon and may be due to surgical removal of ventricular cysts and tumours.[1] We report a case of bilateral fornix infarction with reduced fractional anisotropy values at 3 T after anterior communicating artery aneurysm clipping.

A healthy 33-year-old woman was admitted to our hospital with the incidental finding of an anterior communicating artery (ACoA) aneurysm on magnetic resonance angiography. Neurological examination was normal. Digital subtraction angiography visualised a broad based, tapered and 4 mm sized aneurysm of the ACoA and a median callosal artery (fig 1C). The ACoA aneurysm was treated with surgical clipping because of its irregular configuration. After surgery, the patient was drowsy with fluctuating impaired vigilance. She was disoriented in time, space and person, and revealed anterograde amnesia and amnesic aphasia. Her relatives noticed personality changes, psychomotor slowing and decreased spontaneity of speech and behaviour. Apart from transient mild right sided facial paresis, motor function of the limbs, deep tendon reflexes, sensory and coordinative examination and cranial nerves were normal. During the next 5 weeks of

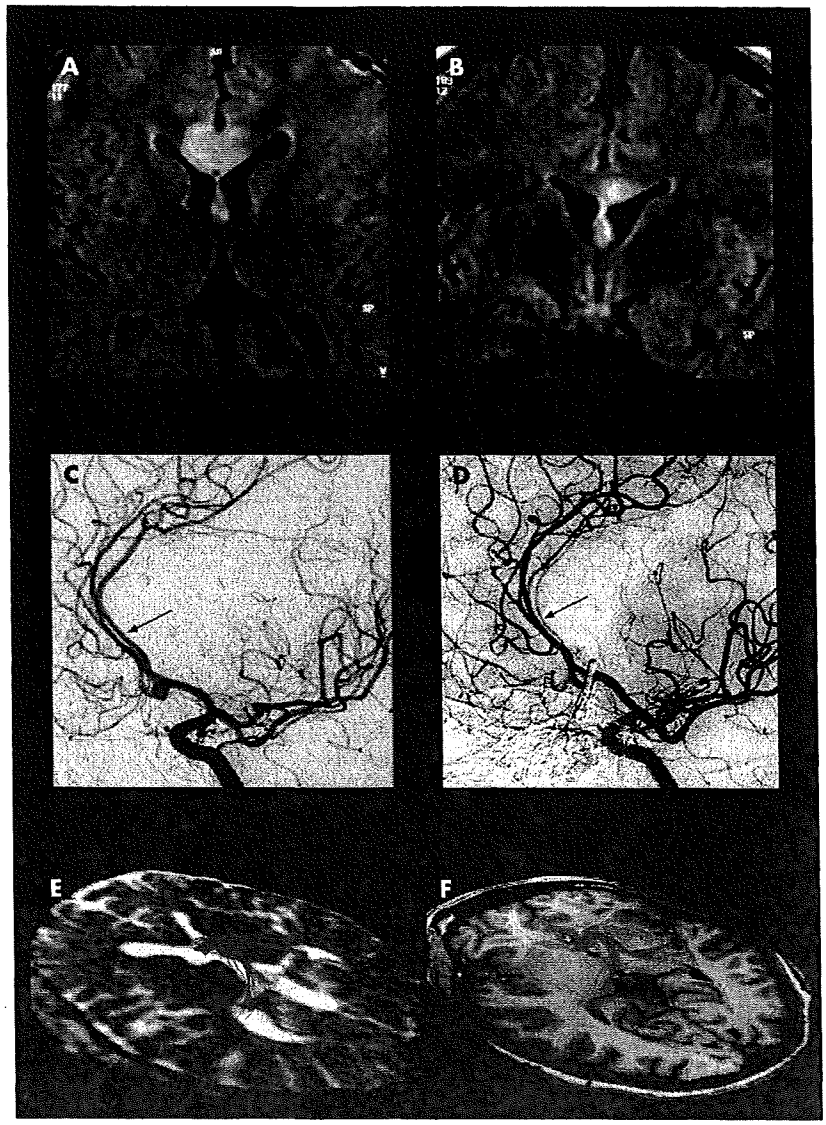


**Figure 1** (A–E) Axial (A) and coronar (B) MRI sections demonstrating a hyperintense lesion on fluid attenuated inversion recovery images of the corpus callosum and the fornix. Initial (C) and postoperative (D) digital subtraction angiography with oblique projection revealed diffuse severe vascular narrowing of the median callosal artery. Fibre tracking of the partially infarcted fornix (E) and in a healthy 34-year-old woman (F). Several erroneous tracts were traced which were excluded in a second step (see frontal fibres on the right).

ANTIOXIDANTS & REDOX SIGNALING
Volume 9, Number 5, 2007

DOI: 10.1089/ars.2006.1522

# Forum Original Research Communication

# Cell Type-Specific Upregulation of Parkin in Response to ER Stress

HUA-QIN WANG,[1,4] YUZURU IMAI,[2,4] AYANE KATAOKA,[3] and RYOSUKE TAKAHASHI[1]

## ABSTRACT

***Parkin* is the gene responsible for a familial form of Parkinson's disease (PD) termed autosomal recessive juvenile parkinsonism (AR-JP)/PARK2. Parkin has been shown to protect cells from endoplasmic reticulum (ER) stress and oxidative stress, presumably due to its ubiquitin ligase (E3) activity that targets proteins for proteasomal degradation. Although the authors showed that parkin is upregulated in response to ER stress, subsequent reports suggest that it does not represent a universal unfolded protein response (UPR). Here the authors report different regulation of parkin in response to ER stress in different cell lines, demonstrating upregulation of parkin as a cell type-specific response to ER stress. 2-Mercaptoethanol (2-ME) and tunicamycin increased the expression of parkin in SH-SY5Y (H) cells, Neuro2a cells, Goto-P3 cells, but not in SH-SY5Y (J) cells and IMR32 cells. In parallel with these studies, similar upregulation of the *parkin* coregulated gene (PACRG)/gene adjacent to *parkin* (Glup) was also observed by ER stress. Luciferase assays failed to detect the transcriptional activation of 500 bp parkin/Glup promoter in response to ER stress. These results indicate that induction of parkin by ER stress represents a cell type-specific response.** *Antioxid. Redox Signal.* 9, 533–541.

## INTRODUCTION

PARKINSON'S DISEASE (PD) is the most common neurodegenerative movement disorder characterized by a progressive loss of dopaminergic neurons in the substantia nigra pars compacta. Most cases of PD are sporadic and the etiology of the disease remains unclear. However, recent identification of genes responsible for relatively rare familial forms of PD, which comprise 5–10% of PD, significantly advanced our understanding of the molecular mechanisms underlying PD (4, 22).

*Parkin* is the gene responsible for autosomal recessive juvenile parkinsonism (AR-JP)/PARK2, the most common form of familial PD (1, 16, 20). Since the identification of *parkin*, many studies focused on elucidating the function of this protein, and it has been shown it can function as an ubiquitin ligase (E3) (27). Emerging data suggest that parkin may protect cells from premature death by targeting misfolded or damaged proteins for degradation via the ubiquitin proteasome pathway (9, 11, 35). The majority of parkin mutations are found to either impair its binding to putative substrates or render its ligase activity defective, thus resulting in a decrease in its activity. Therefore, endoplasmic reticulum (ER) stress [also known as unfolded protein response (UPR) stress] derived from accumulation of misfolded or damaged proteins because of the absence of parkin might represent as a mechanism underlying the dopaminergic neurodegeneration (12, 29, 30). ER stress has also been implicated in α-synuclein- or PD toxins-induced neuronal cell death. Induction of A53T α-synuclein expression induced expression of CHOP

[1]Department of Neurology, Kyoto University Graduate School of Medicine, Kyoto, Japan.
[2]Department of Pathology and Geriatric Research, Stanford University School of Medicine, Palo Alto, California.
[3]BSI, RIKEN, Saitama, Japan.
[4]These authors contributed equally to this work.

and BiP, as well as increased phosphorylation of eIF2α and activation of caspase-12. Most importantly, suppression of ER stress partially protected PC12 cells from α-synuclein-mediated cell death, suggesting that ER stress at least in part, contributes to α-synuclein-induced cell death (28). In addition, numerous changes in genes associated with UPR were identified in toxins-induced PD cell models (6, 25, 34). Moreover, neurons, which generally have small capacity to deal with ER stress by inducing an appropriate UPR are more sensitive to PD mimicking toxins (25). Collectively, these researches raise the possibility of widespread involvement of ER stress in the pathogenesis of PD.

Several studies have implied that the physiological role of parkin may be directly related to unfolded protein stress and the UPR pathway (9, 11). The ER-associated E2 enzymes, Ubc6 and Ubc7, apparently function as collaborating partners of parkin, indicating that parkin acts as part of the ER-associated degradation (ERAD) machinery. We have reported that ER stress caused by accumulation of unfolded protein upregulates parkin mRNA and protein levels, and that overexpression of parkin prevents unfolded protein stress-induced dopaminergic cell death (5, 11). However, there is a discrepancy among these reports on the induction of parkin upon ER stress (5, 11, 18, 21, 32). To clarify this point, we investigated the alteration of parkin expression upon ER stress in a panel of cell lines. The present experiments confirm our previous results that parkin mRNA and protein levels are increased in a subset of cell lines, but not in the rest of the cell lines. Thus, response to ER stress by increasing the expression of parkin appears to be cell-type specific, and inability to upregulate parkin might result in a higher vulnerability to ER stress.

## MATERIALS AND METHODS

### *Plasmids, antibodies, and reagents*

The sequence between human *Parkin* and *Glup* genes was cloned by polymerase chain reaction (PCR) from genomic DNA of SH-SY5Y cells and subcloned into the reporter plasmid pGL4 (Promega, Madison, WI). Anti-Parkin, anti-Glup, and anti-Hdj2 antibodies were described elsewhere (8, 9, 11). Anti-BiP (N-20), anti-Hsp70 (K-20), and anti-Hsc-70 (K-19) antibodies were purchased from Santa Cruz Biotechnology (Santa Cruz, CA). Anti-actin (C4), anti-TCP1α (CTA-184), and anti-tyrosine hydroxylase (TH) (MAB318) antibodies were obtained from Roche Diagnostics (Mannheim, Germany), StressGen (San Diego, CA), and Chemicon (Billerica, MA), respectively. Tunicamycin, 2-mercaptoethanol (2-ME), retinoic acid, 12-*O*-tetradecanoylphorbol 13-acetate (TPA), and $N^6$, 2′-*O*-dibutyryladenosine-3′,5′-cyclic monophosphate (dcAMP) were obtained from Nakalai tesque (Kyoto, Japan). Nerve growth factor 2.5S and MG-132 were purchased from Sigma (St. Louis, MI) and the Peptide Institute (Osaka, Japan), respectively.

### *Cell culture and transfection*

Human SH-SY5Y cell lines were obtained from M. Nomura (Hokkaido University) and N. Hattori (Juntendo University) and termed SH-SY5Y (H) and (J) in this article, respectively. SH-SY5Y and mouse Neuro2a cell lines were maintained in Dulbecco's modified Eagle's medium (DMEM), supplemented with 10% bovine fetal calf serum (FCS). Human GOTO-P3 cells, obtained from RIKEN Cell Bank (Saitama, Japan), were maintained in RPM11640 plus 10% FCS. IMR32 cells, obtained from Cell Resource Center for Biomedical Research (Tohoku University), were maintained in Eagle's minimum essential medium plus 10% FCS and 1 m*M* sodium pyruvate. Transfection was performed with Lipofectamine 2000 (Invitrogen, Carlsbad, CA) according to the manufacturer's instructions. phRluc-TK synthetic renilla vector (Promega) expressing *Renilla* luciferase was also transfected into the cell cultures simultaneously to act as a control for transfection efficiency, in a molar ratio of 1:10 (phRluc-TK vs. pGL4). Twenty-four hours after transfection, the cells were treated with vehicle or ER stress inducers for the indicated time and the transcriptional activities were determined by measuring the luminescent signal produced by the firefly luciferase reporter.

### *Luciferase assay*

The luciferase activity was determined using the Dual-Luciferase ® Reporter Assay System (Promega), according to the manufacturer's user protocol. The activities of firefly (*Photinus pyralis*) and *Renilla (Renilla reniformis)* luciferases were measured sequentially from a single sample. Firefly luciferase activities were normalized by *Renilla* activities to correct for differences in transfection efficiencies. All transfection experiments were repeated at least three times in triplicate. Statistical significance was analyzed by Student's *t* test. Firefly luciferase activities normalized by *Renilla* activities are presented as fold induction relative to the normalized firefly luciferase activity in cells transfected with the pGL4 empty vector only, which was taken as 1.0.

### *Quantitative RT-PCR*

Taqman EZ RT-PCR was carried out as previously described (11). The reverse transcript (RT) parameters (initial step, 50°C 2 min; RT, 60°C 30 min; deactivation for the reverse transcriptase, 95°C 5 min) and thermal cycling parameters (denaturation, 94°C 20 sec; annealing/extension, 62°C 1 min; each 40 cycles) were used according to the manufacturer's protocol. The primers and probe sequences were as follows: human parkin forward primer, 5′-TACGTGCACAGACGTCAGGAG; human parkin priming and reverse primer, 5′-GACAGCCAGCCACACAAGGC; human parkin probe, 5′-CAACTCCCGCCACGTGATTTGCTTAGACTG; human TCP1α forward primer, 5′-AAACTATGCAACCAGCATGGG; human TCP1α priming and reverse primer, 5′-GGGCCTCATTATGAAAAGCTCTT; human TCP1α probe, 5′-TCTCGGGAACAGCTTGCGATTGC; human Glup forward primer, 5′-TCCTCCCTGTCCTGAACATCTT; human Glup priming and reverse primer, 5′-CTCGAAGGCCTCCAGTGTCT; human Glup probe, 5′-TCCGGAGACGGCATTGACTACAGCC; human glyceraldehyde- 3-phosphate dehydrogenase (GAPDH) forward primer, 5′-GAAGGTGAAGGTCGGAGTC; human GAPDH priming and reverse primer, 5′-GAAGATGGTGATGGGATTC; human GAPDH probe, 5′-CAAGCTTCCCGTTCTCAGCC; mouse parkin forward primer, 5′-TGTGGAGCACACCCAACCT; mouse parkin priming and reverse